

Electronic Supplementary Information

Carbon dioxide reduction on Ir(111): stable hydrocarbon surface species at near-ambient pressure

Manuel Corva,^{ab} Zhijing Feng,^{ab} Carlo Dri,^{ab} Federico Salvador,^b Paolo Bertoch,^b Giovanni Comelli,^{ab} and Erik Vesselli^{*ab}

^aPhysics Department, University of Trieste, via Valerio 2, I-34127 Trieste, Italy

^bIOM-CNR Laboratorio TASC, Area Science Park, S.S. 14 km 163.5, I-34149 Basovizza (Trieste), Italy

*E-mail: vesselli@iom.cnr.it

Discussion of the SFG data fitting procedure

In order to guide the discussion, a selected example is reported in Figure S1 (panel a), where the normalized SFG intensity in the C-O stretching region obtained upon exposure of the Ir(111) surface to 10^{-1} mbar CO₂ is reported. At this point, we thoroughly discuss different possible approaches to the visualization of the data fitting results. Going into further detail, the expression for the second-order susceptibility $\chi^{(2)} = \chi_{NRes}^{(2)} + \chi_{Res}^{(2)}$ in Eq. 1 (main paper) can be conveniently rewritten in order to highlight specific quantities of physical and chemical interest. Indeed, the real and imaginary components of the refraction index describe the scattering and absorption properties of a system, respectively, and can be readily obtained for the resonant part:

$$\chi_{Res}^{(2)}(\omega_{IR}) = Re \left[\sum_k \frac{A_k e^{i\varphi_k}}{\omega_{IR} - \omega_k + i\Gamma_k} \right] + i Im \left[\sum_k \frac{A_k e^{i\varphi_k}}{\omega_{IR} - \omega_k + i\Gamma_k} \right] \quad (\text{Eq. S1})$$

and separately represented in an amplitude (not intensity) plot (Figure S1, panel b). Alternatively, the real (Figure S1, panel c) and imaginary (panel d) amplitudes can be displayed for each k^{th} resonance separately

$$\chi_{Res,k}^{(2)}(\omega_{IR}) = Re \left[\chi_{Res,k}^{(2)} \right] + i Im \left[\chi_{Res,k}^{(2)} \right] = Re \left[\frac{A_k e^{i\varphi_k}}{\omega_{IR} - \omega_k + i\Gamma_k} \right] + i Im \left[\frac{A_k e^{i\varphi_k}}{\omega_{IR} - \omega_k + i\Gamma_k} \right] \quad (\text{Eq. S2})$$

thus representing the individual contributions to the resonant amplitudes. The above plotting choices yield alternative visualization possibilities of the information determined with the data least-square fitting procedure and allow speculating about the signal amplitudes.¹ It is indeed known that if N resonances are present in an SFG spectrum, up to 2^N equivalent sets of parameters can be obtained upon data fitting according to Eq. 1.^{2,3} This occurs since we actually measure intensities and not amplitudes. In order to unequivocally determine the real and imaginary components of the resonant susceptibility, phase-sensitive SFG spectroscopy should be exploited.³ Since this is not our case, we here propose and adopt throughout the manuscript a plot of the deconvoluted intensities (not amplitudes) contributing to the effective SFG signal (Figure S1, panel e), thereby avoiding to speculate about amplitudes, but providing visual information about the contribution of each resonance to the overall intensity. For each k^{th} component we therefore display, coherently with the experimental and best fit SFG intensity curves, the following function

$$I_{SFG,k}(\omega_{IR}) \sim \left| A_{NRes} + \frac{A_k e^{i\Delta\varphi_k}}{\omega_{IR} - \omega_k + i\Gamma_k} \right|^2 \quad (\text{Eq. S3})$$

This intensity expression accounts for the interference of each of the resonances with the non-resonant background, while interference among different resonances is not represented. The latter, indeed, is already visualized in the fitting curves according to Eq. 1. With reference to Figure S1, panel (e), the intensity curves are color-filled with respect to the non-resonant background, represented by the horizontal dashed line. The vertical dashed lines show the actual positions of the resonances ($\omega_1 = 2071 \text{ cm}^{-1}$; $\omega_2 = 2080 \text{ cm}^{-1}$) as from the data fitting procedure.

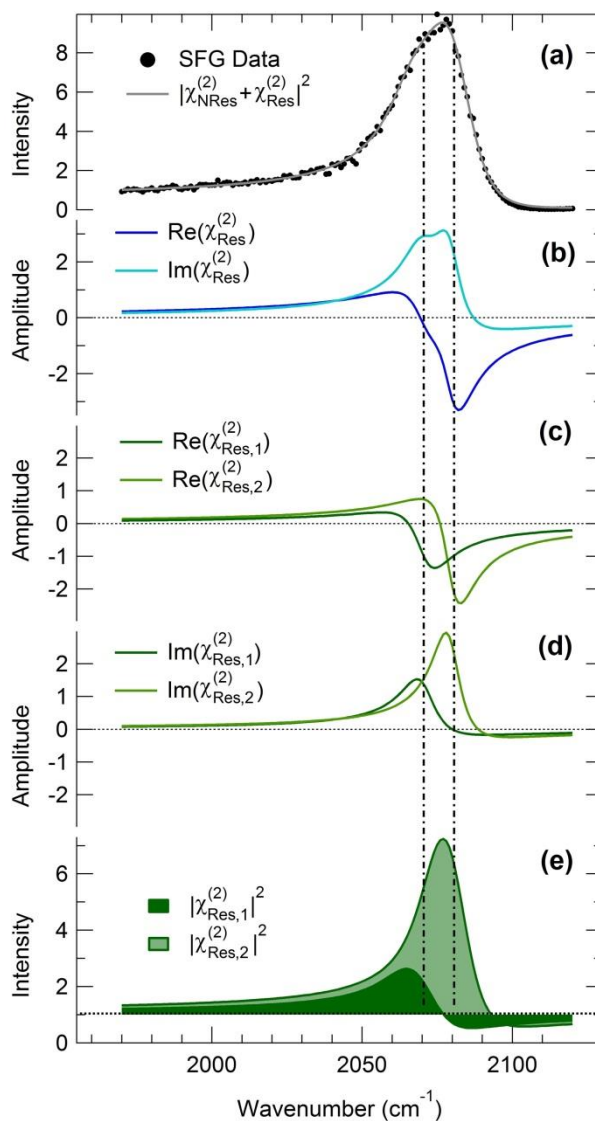


Figure S1. Analysis and interpretation of SFG data: (a) SFG intensity spectrum in the C-O stretching region upon exposure of Ir(111) to CO_2 (dots) and best-fit (grey line) with the function of Eq. 1; as obtained from the least-square fit of the data, (b) shows the amplitude of the real and imaginary parts of the resonant susceptibility (Eq. S1), (c) shows the amplitude of the real part of the resonant susceptibility for each resonance (Eq. S2), (d) shows the amplitude of

the imaginary part of the resonant susceptibility for each resonance (Eq. S2), (e) shows the intensity for each resonance (Eq. S3), color-filled with respect to the non-resonant background (horizontal dashed line); vertical dashed lines show the position of the resonances ω_1 and ω_2 as from the data fitting procedure; amplitude and intensity values (y axis) are in arbitrary units.

We reserve a dedicated discussion to the SFG data fitting procedure adopted for the C-H stretching region, where several features were observed and could be resolved after a careful analysis. In particular, the features at 3000 ± 9 and 3035 ± 6 cm^{-1} (cyan and light blue in Figures S2 and S3) may be attributed at first glance to a single vibrational mode with a dispersive lineshape, in analogy to the peak at 2904 ± 3 cm^{-1} (dark red curve in Figure S2), i.e. in phase quadrature with respect to the non-resonant background.

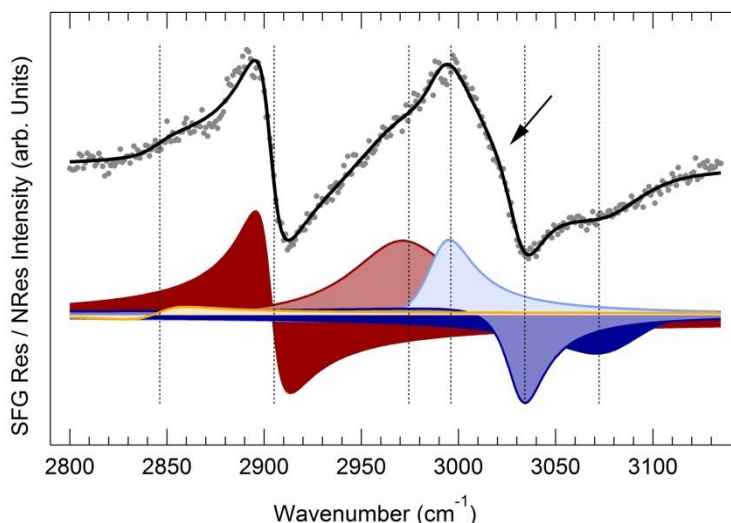


Figure S2. Deconvolution of the C-H stretching region: selected example. The arrow indicates an evident “knee” in the spectrum requiring two distinct peaks to reproduce the data, instead of a single dispersive lineshape. Vertical dashed lines indicate the line-positions.

However, the presence of an evident “knee” in the spectrum (arrow in Figure S2) indicates that two distinct peaks are needed to properly describe the data in that energy region. Indeed, a single dispersive lineshape yields a structured residual and a high chi-value in the least-square fitting analysis. Only with the introduction of two peaks with almost opposite phase the experimental data could be properly reproduced.

Full IR-Vis SFG data set in the C-H stretching region for the carbon dioxide reduction reaction.

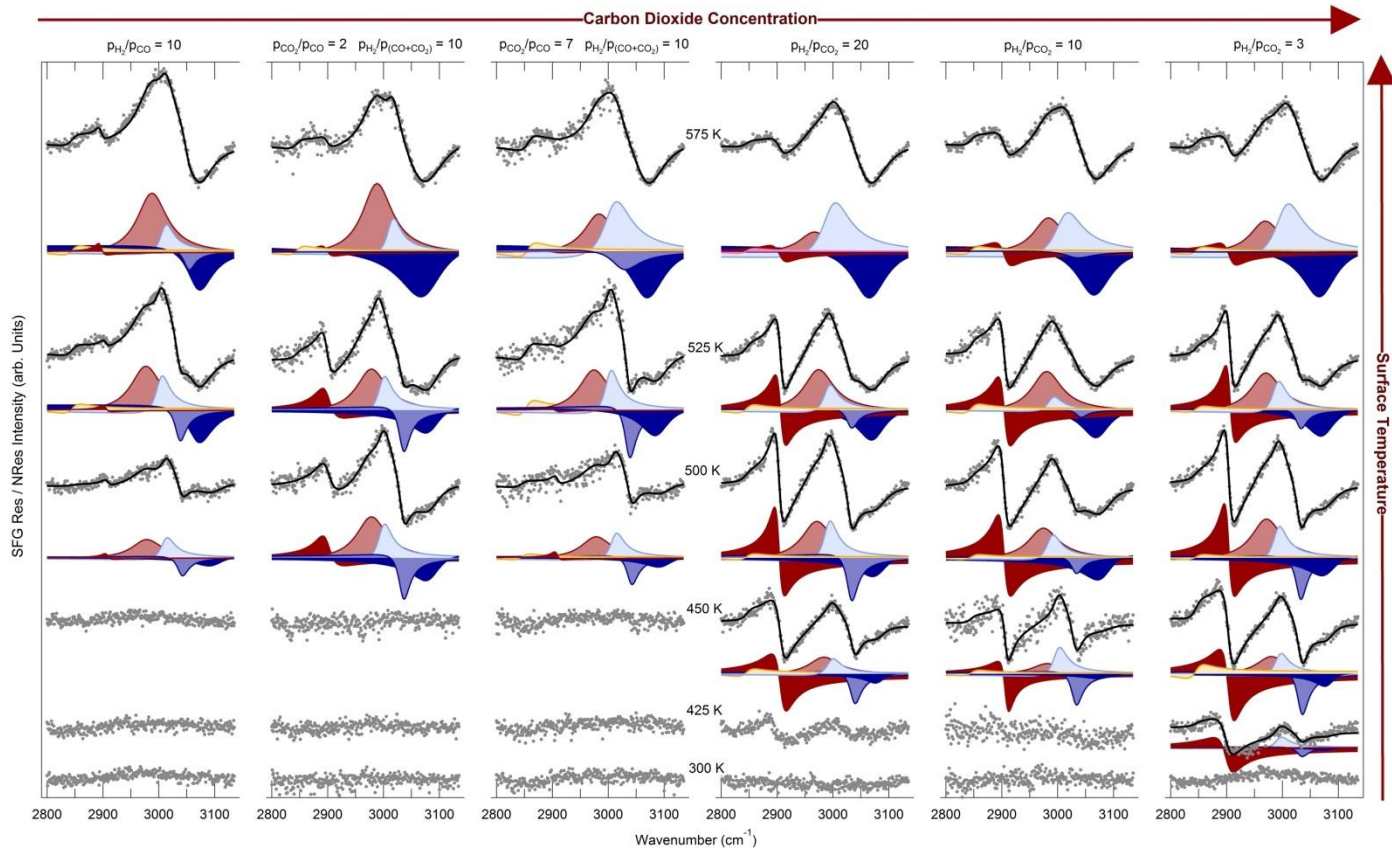


Figure S3. IR-Vis SFG spectra in the C-H stretch region obtained upon annealing the Ir(111) surface exposed to different reactants' partial pressures at 10^{-1} mbar. Data (grey dots) and the results of the least square fitting (black curves) are shown. Colored curves represent deconvoluted intensity modulations with respect to the non-resonant background. [$\lambda_{Vis} = 532$ nm; p-p-p polarization]

Fitting parameters of the IR-Vis Spectra (selected representative spectra).

The best fitting parameters' values obtained from the least-square analysis of the SFG data according to the function described in the text are reported in the following tables (Tables S1-S3). While phase and lifetime parameters were obtained from a global fit of the data and were therefore fixed for each data set, the remaining parameters were instead fitted separately for each curve, yielding, in the case of the analysis of the C-O region, error bars of $\Delta\omega = 2 \text{ cm}^{-1}$, $\Delta(A_k/A_{NR})/(A_k/A_{NR}) = 5 \%$, and $\Delta\omega_G = 2 \text{ cm}^{-1}$ respectively. For the C-H region, ranges are given, the exact parameters' values depending on the different reaction conditions.

Experiment	Figure-panel in Main Text	Temperature (K)	IR Resonance (cm^{-1})	Res/NRes Signal ratio	Lifetime (cm^{-1})	Phase ($^\circ$)	Gaussian Broadening (cm^{-1})
CO ₂	1-left	300	2080	26	6	32	4
			2071	16	7	37	4
		500	2060	27	6	32	5
			2050	19	7	37	5
CO	1-right	300	2026	26	24	32	-
			2079	43	6	32	6
		500	2064	49	6	32	6
		575	2016	21	21	28	-

Table S1. Best IR-Vis SFG fitting parameters' values for CO₂ and CO adsorption at 10⁻¹ mbar on Ir(111), C-O stretching region.

Experiment	Figure-panel in Main Text	Temperature (K)	IR Resonance (cm^{-1})	Res/NRes Signal ratio	Lifetime (cm^{-1})	Phase ($^\circ$)	Gaussian Broadening (cm^{-1})
H ₂ +CO	3-left	300	2083	53	6	32	4
			450	2072	55	6	32
		525	2033	13	6	32	6
			2019	4.9	7	37	6
H ₂ +CO ₂ +CO	3-center	300	2079	31	6	32	5
			2069	12	7	37	5
		450	2067	34	6	32	5
			2054	11	7	37	5
		500	2038	24	6	32	10
	2016	4	7	37	10		
H ₂ + CO ₂	3-right	300	2077	30	6	32	4
			2069	19	7	37	4
		450	2039	32	6	32	7
			2011	2.6	7	37	7

Table S2. Best IR-Vis SFG fitting parameters' values for the reduction experiments at 10⁻¹ mbar on Ir(111), C-O stretching region.

IR Resonance Range (cm ⁻¹)	Res/NRes Signal ratio	Lifetime (cm ⁻¹)	Phase Range (°)
2845 ± 3	0.0 - 1.1	16	185
2904 ± 3	0.0 - 4.6	11 ± 3	357 ± 18
2976 ± 6	0.0 - 9.6	33	265
3000 ± 9	0.0 - 7.1	18 ± 6	240
3035 ± 6	0.0 - 3.3	16 ± 7	68
3078 ± 10	0.0 - 10.5	31 ± 6	107 ± 18

Table S3. Best IR-Vis SFG fitting parameters' values (ranges, values depending on reaction conditions) for the reduction experiments at 10⁻¹ mbar on Ir(111), C-H stretching region.

Ethylene adsorption and dissociation on Ir(111) monitored by IR-Vis SFG.

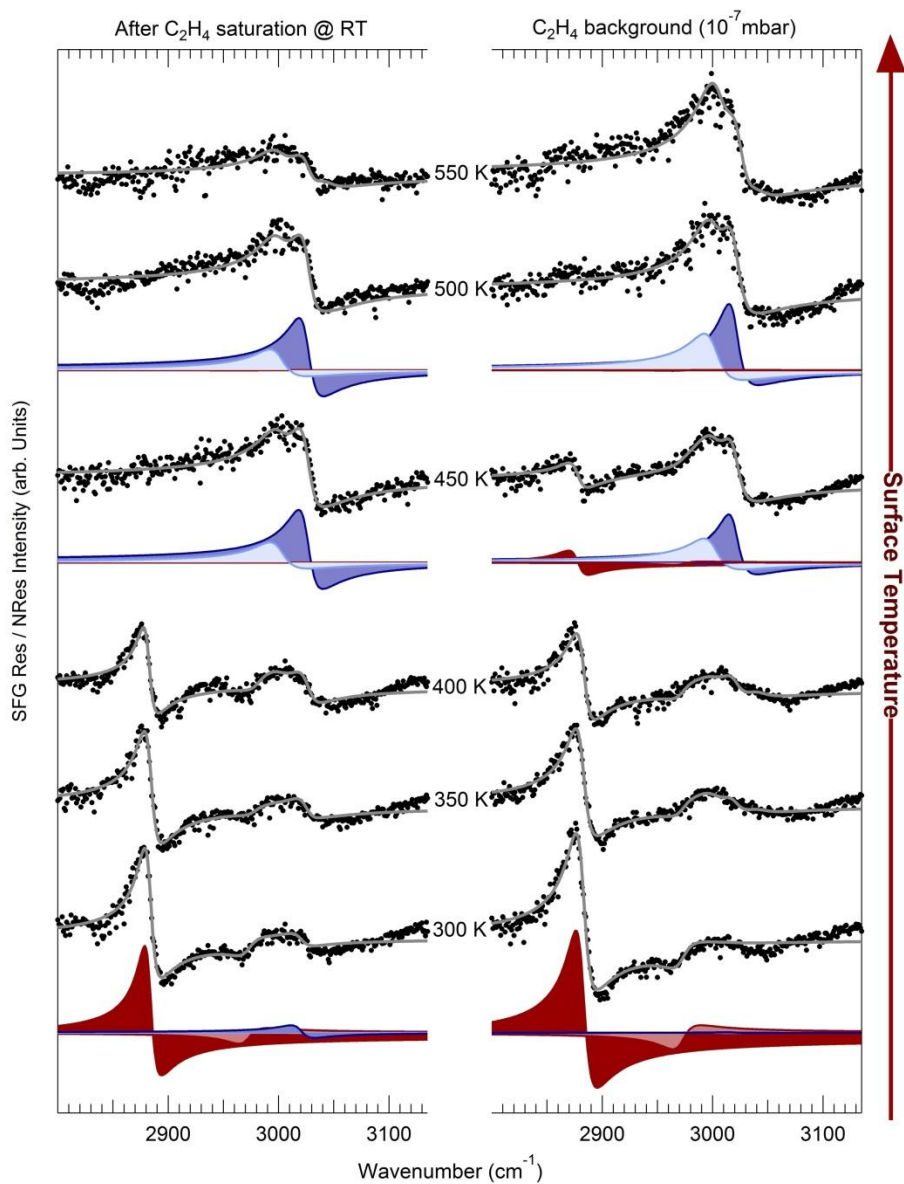


Figure S4. IR-Vis SFG spectra in the C-H stretch region obtained upon annealing the Ir(111) surface after ethylene saturation at RT (left) and in constant ethylene background (right). Data (grey dots) and the results of the least square fitting (black curves) are shown. In selected cases, colored curves represent deconvoluted intensity modulations with respect to the non-resonant background. [$\lambda_{\text{vis}} = 532 \text{ nm}$; p-p-p polarization]

Upon exposure to ethylene of the Ir(111) surface, four main spectral features can be identified in the C-H stretch region at 2880 ± 3 , 2975 ± 5 , 3002 ± 2 , and $3023 \pm 3 \text{ cm}^{-1}$. This chemical treatment is widely used to grow a well ordered, almost free standing, graphene sheet

on this surface under UHV conditions. According to the literature,⁴ on the basis of high-energy resolution XPS data, the main intermediate present on the surface in the RT - 400 K temperature interval can be identified with ethylidyne (CCH_3), while at higher temperature two non-equivalent ethynyl species (CCH) are reported to be present up to the complete dehydrogenation of the layer occurring at about 700 K, yielding formation of carbon and progressive networking to form graphene. In HREELS spectra a broad feature in the 2940-2960 cm^{-1} range is obtained upon adsorption and decomposition of ethylene or acetylene on Ir(111) and is ascribed to the asymmetric stretching mode of the methyl group of an ethylidyne intermediate.⁵ On Pt(111) the same mode is observed at 2939 cm^{-1} .⁶ Analogously, on platinum and palladium single crystal terminations the symmetric mode of ethylidyne is observed (by means of SFG, FT-IRAS, and RAIRS) in the 2870-2890 cm^{-1} range.⁶⁻¹⁰

On the basis of these data, we conclude that the two low energy features that we observe below 400 K (red curves) can be ascribed to the symmetric ($\omega = 2880 \pm 3 \text{ cm}^{-1}$, $\Delta\phi = 355 \pm 5^\circ$) and antisymmetric ($\omega = 2975 \pm 5 \text{ cm}^{-1}$, $\Delta\phi = 155 \pm 20^\circ$) stretching modes of the methyl groups of adsorbed ethylidyne, respectively. The other two features at higher energy (blue curves; $\omega = 3002 \pm 2 \text{ cm}^{-1}$, $\Delta\phi = 330 \pm 5^\circ$; $\omega = 3023 \pm 3 \text{ cm}^{-1}$, $\Delta\phi = 340 \pm 10^\circ$) are instead due to the stretching of non-equivalent ethynyl species, according to the photoelectron spectroscopy assignment,⁴ and on the basis of the vibrational fingerprint of ethynyl intermediates previously observed on Ir(111) and Pt(111) surfaces.^{5,6} It is also to be noted that a broad feature (right panel, not fitted) develops progressively at the high energy side of the spectrum with increasing temperature, appearing as a depression in the spectra and shifting from 3040 to 3080 cm^{-1} while heating. This pattern is present up to 700 K (not shown), when complete dehydrogenation of the surface occurs and, as reported in the literature, dome-shaped carbon nanoislands develop as intermediates between carbidic clusters and quasi-free standing graphene.¹¹

References

- 1 M. Ito, H. Noguchi, K. Ikeda and K. Uosaki, *Phys. Chem. Chem. Phys.*, 2010, **12**, 3156.
- 2 B. Busson and A. Tadjeddine, *J. Phys. Chem. C*, 2009, **113**, 21895–21902.
- 3 Y. R. Shen, *Annu. Rev. Phys. Chem.*, 2013, **64**, 129–150.
- 4 S. Lizzit and A. Baraldi, *Catal. Today*, 2010, **154**, 68–74.
- 5 T. S. Marinova and K. L. Kostov, *Surf. Sci.*, 1987, 181, 573–585.
- 6 R. Deng, E. Herceg and M. Trenary, *Surf. Sci.*, 2004, **573**, 310–319.
- 7 M. Morkel, G. Rupprechter and H.-J. Freund, *Surf. Sci.*, 2005, **588**, L209–L219.
- 8 K. R. McCrea and G. a Somorjai, *J. Mol. Catal. A Chem.*, 2000, 163, 43–53.
- 9 P. Cremer, C. Stanners, J. W. Niemantsverdriet, Y. R. Shen and G. Somorjai, *Surf. Sci.*, 1995, **328**, 111–118.
- 10 I. J. Malik, V. K. Agrawal and M. Trenary, *J. Chem. Phys.*, 1988, **89**, 3861–3869.
- 11 P. Lacovig, M. Pozzo, D. Alfè, P. Vilmercati, A. Baraldi and S. Lizzit, *Phys. Rev. Lett.*, 2009, **103**, 166101.